XIX IMEKO World Congress
Fundamental and Applied Metrology
September 6−11, 2009, Lisbon, Portugal

ABSOLUTE CALIBRATOIN OF OPTICAL FLATS THROGOUT THE SELF COMPARISON AND IMAGE PROCESSING

Sánchez Jose [1], *Ruiz Gerardo* [2], *Padilla Sergio* [3], *Valera Benjamín* [4]
[1,3,4] Precision Engineering Laboratory, CCADET, Universidad Nacional Autónoma de México,
jose.sanchez@ccadet.unam.mx, sergio.padilla@ccadet.unam.mx, benjamin.valera@ccadet.unam.mx
[2] Instrumentation & Measurement Department, CCADET, Universidad Nacional Autónoma de México,
gerardo.ruiz@ccadet.unam.mx

Abstract – Optical flats are required for spreading accuracy to mechanical and optical instruments, ordinarily by optical interference. Traceability of optical flats is ordinarily made by Fizeau interferometer. Traceability of this one requires higher accuracy flats, not available in secondary laboratories. These laboratories can accede to absolute self-calibration principles, by a method proposed by Bernard [1], who compares three flats among them through Zernike polynomials [2], representing these last their topographies.

Two problems are found when the process is intended to set up: (a) the Zernike polynomials have not easy geometric meaning and direct equivalence with CAD entities; (b) neither fringes nor levels of gray of interferograms have direct equivalences with the shape of flats or virtual membranes.

For modelling shapes we adopted the self calibration concept of Bernard, but using b-splines models with ring shape, instead Zernike. This substitution offer important algebraic simplifications and possibilities for exporting shapes to CAD; supporting validation.

For converting interferograms to shapes of membranes, three major problems are present: the aspect of patterns, the ambiguity in inflection areas, and the adequate interpretation of gray scales.

After applying low pass filters to brightness, two methods were applied: (a) heuristic genetic, (b) inverse sine correlation of gray for relief. Success in interpretation of shape have been by now better than 75%.

Keywords: Self-calibration, optical flats, interpherograms conversion

1. INTRODUCTION

1.1 Motivation

Traceability in flatness is not absolutely necessary, since it is a geometrical property, and not a quantity established by agreement, as the second or the meter are. The traceability of maser flats with primary laboratories, results long and expensive. It is very useful then, a method for self calibration.

On the other hand, comparison of flats by interference, when is made by man, ordinarily give out deviations of some points only, and not a continuous relief. Then a level of automation for getting complete and continuous information from interpherograms is required.

1.2 Principles used on self calibration

For making high accuracy flats, three pieces are lapped each other; if they are convex or concave, only a pair will match, but not a third one. In mechanics peaks will produce abrasion, smoothing them. In optics peaks will interfere, producing patterns of fringes. In both cases the absence of flatness are revealed, constituting a method of self calibration.

A first intent to correlate information from optical comparison, is supposing that geometric differences of flats are ready. Using the model of Bernard, these differences are *D, E, G* as in equations (1). They are produced when flats *k, l, m* are compared. See fig. 1 and Equation 1.

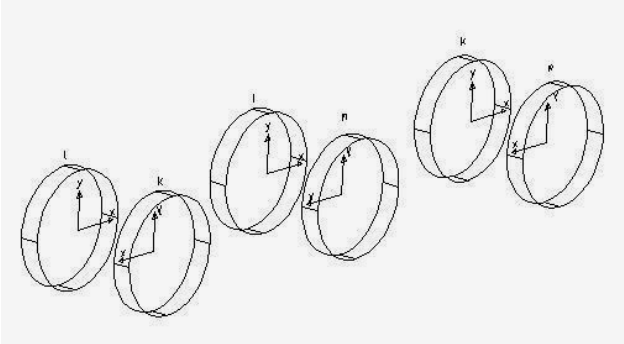

Fig. 1. *Flats and axis of reference when compared.*

$$\begin{aligned} k(x,y)+l(-x,y) &= D(x,y) \\ m(x,y)+l(-x,y) &= E(x,y) \\ m(x,y)+k(-x,y) &= G(x,y) \end{aligned} \qquad (1)$$

These may be solved for cases with left - right symmetry, which occur when $x = 0$, according system (2).

$$m(x,y)=\frac{-D(x,y)+E(x,y)+G(x,y)}{2}$$
$$l(x,y)=\frac{D(x,y)+E(x,y)-G(x,y)}{2} \quad (2)$$
$$k(x,y)=\frac{D(x,y)-E(x,y)+G(x,y)}{2}$$

But for regions x ≠ 0, equations (2) are not valid since *D(x, y) ≠ D(-x, y)*; and so for *E, G*.

For translating the true values obtained along the axis *Y*, Bernard rotates the *m* flat, and compared again with *l*, obtaining a new interpherogram *F*:

$$m(x,y)_{ROT\phi}+l(-x,y)=F(x,y) \quad (3)$$

From here after, the shape of the line along axis $Y_{ROT\phi}$ of *m* is spread to *l, k,* which once again the information is feed-backed to other region of *m*. To perform the comparison Zernike polynomials are normally adopted.

Although Zernike offers useful information for optical applications, geometrical polynomials look friendlier for dimensional metrology, for mechanical correction, or for simulation.

2. MODELLING WITH B-SPLINES

The simplest case of a b-spline is a Bezier curve which is shaped by *Vi* vertexes, throughout blending functions *Bi, n*, along a parameter *u*: 0. <= *u* <= 1, as describe by (4) [3].

$$p(u)=\sum_{i=0}^{n} V_i B_{i,n}(u) \quad (4)$$

2.1 Useful characteristics of b-splines

Geometric and algebraic symmetry is possible to perform when vertexes are arranged inversely as (5).

$$p(1-u)=\sum_{i=n}^{0} V_i B_{i,n}(1-u) \quad (5)$$

If values of vectors *Vi* are changed in sign or in the order, we get mirror or symmetrical curves. Those characteristics of symmetry may be used to establish correlations with geometrical and algebraic meaning at once.

Keeping their characteristics of symmetry, the polynomials may be transformed into b-splines 2nd degree as represented in (6).

$$p(u_i)=\begin{bmatrix}\frac{(1-u_i)^2}{2} & \frac{1+2u_i-2u_i^2}{2} & \frac{u_i^2}{2}\end{bmatrix}\begin{bmatrix}V_{i-1}\\ V_i\\ V_{i+1}\end{bmatrix} \quad (6)$$

If the curve has five or more vertex, and the last two final vertexes *Vi, Vi+1*, coincide with the first and second ones, the curve is closed and continuous. The location of vertexes may be periodic as in regular polygons. For twelve or more vertexes, the curve is closer to the circle. In this assumption of location, the only free parameters will be the high of *Vi*, named *Zi*.

For describing thin rings as surfaces, two sets of vertex will describe them with the equation (7).

$$p(u_i)=\begin{bmatrix}\frac{(1-u_i)^2}{2} & \frac{1+2u_i-2u_i^2}{2} & \frac{u_i^2}{2}\end{bmatrix}\begin{bmatrix}V_{i-1} & W_{i.-1}\\ V_i & W_i\\ V_{i+1} & W_{i+1}\end{bmatrix}\begin{bmatrix}1-v\\ v\end{bmatrix} \quad (7)$$

For representing the ring in a rotated position, only one operation of rotation is required. If rotation coincides with frequency of polygons, it may be made by changing the order *i* of vertexes.

Concentric rings modelled with (7) may model all flats. But collection of concentric rings modelled as wires with (6), may also be edited by CAD commands, to configure entire flats or membranes. This last procedure was adopted.

2.2. Applying b-splines to the process

The *u* variable in (6) will vary with ø in steps, for each segment of polygon of *n* vertex.

The correlation of flats with rings shape is done with (8), where we have won polar symmetry:

$$\begin{aligned} k(\theta)+l(-\theta)&=D(\theta)\\ m(\theta)+l(-\theta)&=E(\theta)\\ m(\theta)+k(-\theta)&=G(\theta)\\ m(-\theta-\phi)+l(\theta)&=F(\theta)\end{aligned} \quad (8)$$

Since the high of curves and their vertexes have linear relation, the equation (8) may be written as (9) if ø coincide with a step of the polygon.

$$\begin{aligned} Zl(i)+Zk(N+1-i)&=ZD(i)\\ Zm(i)+Zl(N+1-i)&=ZE(i)\\ Zm(i)+Zk(N+1-i)&=ZG(i)\\ Zl(i)+Zm(N-i)&=ZF(i)\end{aligned} \quad (9)$$

Where all unknown parameters are the high *Z* of vertexes: *Zl(i), Zm(i), Zk(i): i=1 to n*.

Solution of (9) may be done with the recurrence (10):

$$\begin{aligned} &Zm(1)=\frac{ZG(1)-ZD(1)+ZE(1)}{2}\\ &i=1, \quad \rightarrow \quad n/2-1\\ &Zm(n-i+1)=ZG(i)-ZD(i)+ZE(i)-Zm(i)\\ &Zm(i+1)=ZG(n-i+1)-ZD(n-i+1)+ZF(n-i+1)-Zm(n-i+1)\\ &next \quad i\end{aligned} \quad (10)$$

2.1 Results of modelling and simulation

Figure 1 represents the process of comparing virtual membranes and their solution when modelled with rings. The *D* membrane is inverted top-down for comparison. Note that transportation to CAD is done directly, supporting validation.

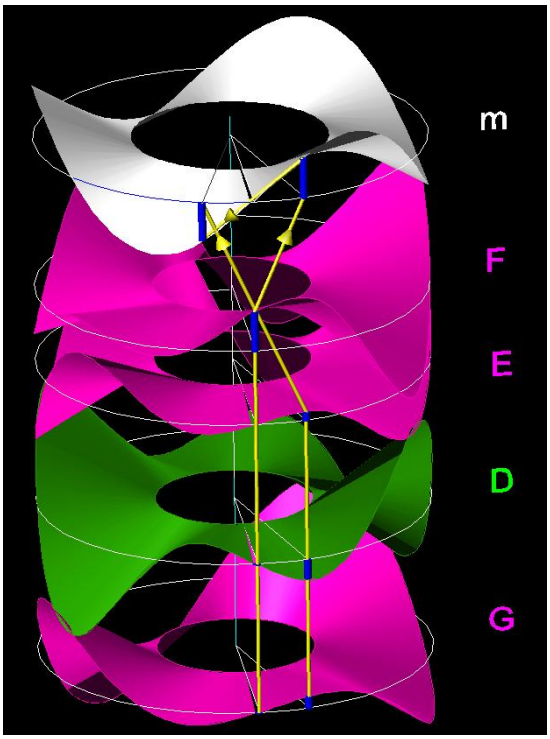

Fig. 1. Testing the process. The right yellow line represents the first equation of loop (10); the left represents the second one.

3. OBTAINING VIRTUAL MEMBRANES FROM INTERFEROGRAMS

The virtual membranes to be compared with (1), (8), (9) are not ready from the interpherometer. Some properties of fringes may be used to obtain them: curvature, distribution, levels of gray, and their likelihood with synthetic ones.

3.1 Pre-processing.

A general process able to interpret any interpherogram, must be immune to noise, variations on brightness, echoes, second reflections, islands and discontinuities of fringes.

Cameras used to catch natural scenario convert the power of light, ordinarily from 10 to 100 k lux, to 255 levels. On the other hand, the periodicity of fringes lets assume that shadows must follow sine distribution. Processors for normalizing the brightness were developed.

Although flats to be calibrated and models for comparison have circular aspect, pre-processing is easier to do on rectangular patterns than on circular. Processors for bidirectional mapping from circular to rectangular were developed. Real interpherograms have echoes and small islands of noise; low pass filters to eliminate them were developed.

Figure 2 shows a sequence of pre-processing. Principles of filtering applied to last image are both: sine variation with location, and global sine distribution of gray on histograms.

Spurious shades on last picture derive from discontinuities of fringes or islands; and they were included to show the range of difficulties that appear when an automated process of images is intended to set up.

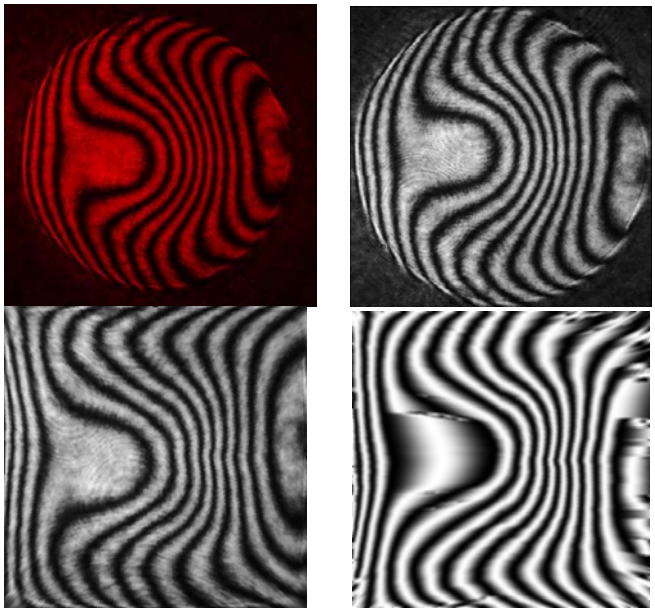

Fig. 2. Sequence where image are colour converted, scaled, squared, and sine gray filtered.

3.1 Searching the shape with genetic algorithms.

After interpherograms have been filtered, some techniques for comparing them with synthetic ones may be applied.

The goodness of likelihood was established as:

$$Good = \frac{1}{Wide * High} \sum_{\substack{j=1 \\ i=1}}^{\substack{High \\ Wide}} (255 - \left| br\,real(i,j) - br\,synt(i,j) \right|) \tag{11}$$

Where:

brreal(i, j) is the brightness of pixel *i, j*, corresponding to real image, from 0 to 255.

brsynt(i, j) is the brightness of pixel *i, j*, corresponding to synthetic image.

i, j are the sub indices corresponding to location of each pixel in the array.

Following genetic techniques, a population of two hundred b-splines (meshes with 49*49 knots) was modified along many hundred of generations.

If Goodness reaches 190, the convergence becomes faster, reaching 220 – 250. When Goodness of a mesh is near to 200, it looks as the second in fig. 3.

It is important to appoint that linear variations of shape produce periodic variations on the pattern; then the matting between good individuals but different among them has not sense. In this application of genetic techniques, the evolution produced better results than the mating.

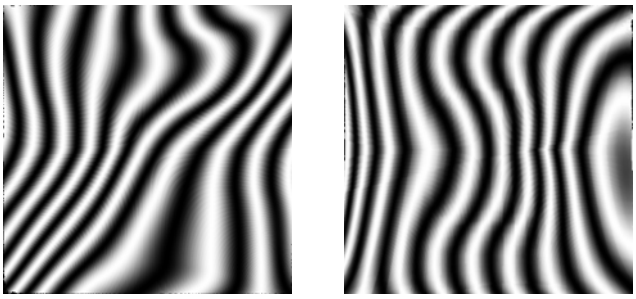

Fig. 3. Synthetic interpherograms where genetic techniques have converged.

3.2 Surveying on surfaces.

After square-circular conversion is made, it is possible to survey along rings, applying the correlation (12)

$$h = \frac{sen^{-1}(\frac{Br}{255} - 1)}{2\lambda} + \frac{N\lambda}{2}, \quad N = 1,2,, \qquad (12)$$

But each function *sine-1(gray)* has two values of angle, on depending on direction where brightness increases.

More cases of ambiguity are: (a) when a point of inflection occurs in full dark or full light fringes, (b) when local small spurious shades appear, (c) when the level of gray does not follow a sine distribution.

Hypothesis of inflection are established, and confirmed through the likelihood with adjacent rings. See fig. 5.

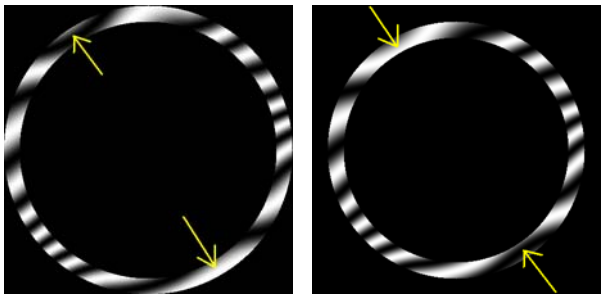

Fig. 5. Adjacent rings show probable inflection areas, where darkness or brightness didn't reach a minimum or maximum.

The level of success when gray is interpreted as high, was better than 90% for synthetic images; and 50% for real.

4. CONCLUSIONS

The simplification proposed with b-spines, did easier the tasks of comparison, offering CAD alternatives for validation.

We appreciate that tools developed for interpreting interpherograms discussed here in, are useful for many applications based on images with noise, where *sine-1* correlations have to be applied.

5. REFERENCES

[1] Bernard S. Fritz, Absolute calibration of an optical flan, OPTICAL ENGINEERING / July/Aug. 1984, Vol. 23, N. 4, 379-383.

[2] Zernike Fritz, John Midwinter, Applied nonlinear optics, J. Wiley NY, 1973.

[3] Michael E. Mortenson, Geometric Modelling, Jhon Wiley & Soons. 1985. ISBN 0-471-88279-8.